Effect of Electrodepositing Voltage on the Structural and in Vitro Corrosion Properties of CaP Coatings on ZK60 Magnesium Alloy

Caiwen Ou[2], Wei Lu[1,*], Zailei Zhan[1], Ping Huang[1], Biao Yan[1] and Minsheng Chen[2,*]

[1] School of Materials Science and Engineering, Shanghai Key Lab. of D&A for Metal-Functional Materials, Tongji University, Shanghai 200092, China
[2] Southern Medical University, No.1023, Shatai Nan Road, Guangzhou City, Guangzhou 510515, China
*E-mail: weilu@tongji.edu.cn; gzminsheng@vip.163.com

CaP coating was successfully prepared on the ZK60 magnesium by electrodeposition. The CaP coatings show a DCPD phase structure with small amount of β-TCP phase. The surface morphology shows a typical dendritic structure and the deposition voltage has little influence on the Ca/P ratio. The corrosion resistance of ZK60 alloy is obviously improved after coated with CaP coatings and the sample with CaP coating deposited at 4V has the best corrosion resistance. The improvement in corrosion resistance will greatly reduce the initial biodegradation rate of the implants, and is essential for maintaining the implant's mechanical strength in the bone reunion period.

1. INTRODUCTION

Magnesium and its alloys have attracted much attention as a biodegradable implant material due to their good biocompatibility and biodegradability recent years [1,2]. Unlike traditional permanent implants, magnesium alloys will not cause permanent physical irritation and stress shielding effect [2, 3]. Magnesium and its alloys degrade in aqueous environments via an electrochemical reaction producing magnesium hydroxide and hydrogen gas [2]. Especially in vivo where the chloride content of the body fluid is about 150mmol/l (which has exceeded the critical concentration 30mmol/l), the degradation rate is faster due to the magnesium hydroxide converts into highly soluble magnesium chloride [4-6]. The rapid degradation rate of the magnesium-based implants in vivo has

become the main limitation hindering their applications [7]. Suitable strategies are thus required to be developed to tailor their degradation rates.

Surface modification is an effective way to improve the biodegradation property as well as the biocompatibility of Mg alloys. [8-13] Calcium phosphates, the major composition of bone, have demonstrated high biocompatibility, osteoconductivity and non-toxicity in an in vivo environment.[12-16] Such evidence advocates that bioactive CaP coating on Mg alloys might be an effective way to solve this problem. Though many methods for fabricating CaP coatings are available, electrochemical deposition (ED) methods are widely used for coating calcium phosphates on metallic implants [17-19], due to their ease of operation and practicability for coating complex structures. Recently, ED methods have been applied for coating calcium phosphates on magnesium alloys [20-22]. However, there are no studies which investigate the effect of electrodepositing voltages on the structural and in-vitro corrosion properties of CaP coatings on magnesium alloys in the literatures.

For avoiding the fast degradation of pure Mg and improving the mechanical properties, 5.5 wt.% zinc and 0.5 wt.% Zr were picked up as the alloy elements in our biodegradable magnesium alloy (ZK60, Mg-5.5wt%Zn-0.5wt%Zr). Zinc is recognized as a highly essential element for humans. In zinc deficiency, nearly all the physiological functions are strongly perturbed. Zirconium possesses a set of suitable properties for orthopedic applications such as low specific weight, high corrosion resistance, and biocompatibility. [12]

In this paper, CaP coatings were electrodeposited onto ZK60 magnesium alloy substrates. The structure, composition and in vitro corrosion properties of the CaP coatings on ZK60 alloy were investigated by changing different depositing voltage, in order to optimize the fabricating procedure of CaP coatings on Magnesium alloys.

2. EXPERIMENTAL

2.1 Sample Pretreatment

The magnesium alloy used in this study was ZK60 alloy, with the major alloying elements of approximately 5.5wt% Zn and 0.5wt% Zr. It was cut into rectangular samples with a size of $10\times10\times5mm^3$. These samples were ground with SiC papers up to 800#, rinsed ultrasonically in ethanol and then air dried.

2.2 Electrodeposition

The experimental set up used for the electrodeposition was a simple two-electrode cell configuration. The working electrode was the ZK60 alloy and the counter electrode was a platinum sheet. Both electrodes were immersed in a supersaturated electrolyte (SE) which was prepared by dissolving given amounts of reagent-grade chemicals $Ca(NO_3)_2 \cdot 4H_2O$, $NH_4H_2PO_3$ and H_2O_2, in demineralized water. The ion concentrations of electrolyte are listed in Table 1. The electrodeposition was carried out at 30 °C while the voltage was changed from 2V to 8 V.

Table 1. Composition of electrolyte solution

Component	Concentration (/L)
$Ca(NO_3)_2 \cdot 4H_2O$	0.1 mol
$NH_4H_2PO_3$	0.06 mol
$30\% H_2O_2$	15~20 mL

2.3 Surface Characterization

The crystallographic structure and chemical compositions of the coatings were examined using X-ray Diffraction (XRD) and energy dispersive spectroscopy (EDS), respectively. To study the morphology, coated samples were analyzed with a field emission scanning electron microscope (FE-SEM).

2.4 Electrochemical Measurements

Corrosion behavior of the samples was studied by electrochemical tests (Tafel Plot) with a electrochemical work station. The experiments were performed in the simulated body fluid (SBF) solution (listed in Ref.12) with a pH value of 7.4 at 37 °C. A three electrode set-up with a saturated calomel reference and a platinum counter electrode was used. The area of the samples for working electrode was $10 \times 10 mm^2$. Prior to characterization, the samples were immersed in the solution for 20 min to establish the open circuit potential.

2.5 Immersion Tests

In vitro immersion tests were carried out in SBF solution. The pH value was adjusted to 7.4 ± 0.1 and the temperature was kept at 37 ± 0.5 °C using a water bath. The samples were immersed into 120 ml SBF solution for 8 days, respectively. The pH value of the solution and the samples' mass were recorded during the immersion every 24h, with a blank SBF solution as control group.
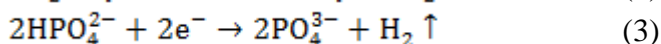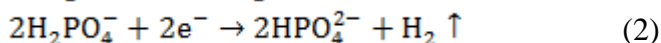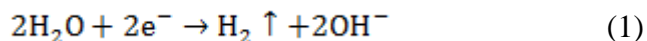
3. RESULTS AND DISCUSSION

3.1 XRD patterns

Fig.1 shows the XRD results of ZK60 alloys with CaP coatings electrodeposited at different voltages. The diffraction peaks from CaP phase and ZK60 substrate can be clearly observed. The patterns show strong peaks at diffraction angle 2θ of 12°, 21° and 29°, which are typical diffraction peaks of DCPD (CaHPO4 · 2H₂O, PDF 72-1240). It can be seen that with increasing voltage, the peak intensities of DCPD phase increase. This is mainly caused by the thicker DCPD coatings at higher
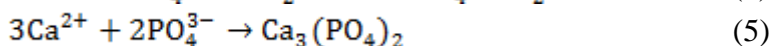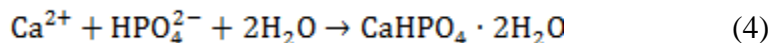
depositing voltage. The peak intensity of DCPD phase gets maximum at voltage of 6V and then decreases when the voltage increases to 8V. This may be explained that high depositing voltage leads to rapid deposition of DCPD phase, which results in poorly distributed DCPD phase. Also, weak peaks of β-TCP (tricalcium phosphate, $Ca_3(PO_4)_2$) are indexed in the coatings from the XRD patterns. Thus, it can be clarified that the CaP coatings are composed of DCPD phase and a small amount of β-TCP phase. It can be seen that there is no significantly changes in the patterns of samples electrodeposited at different voltages. But the peak intensities of β-TCP phase get strongest at 6V. This indicates that part of the DCPD phase transforms to β-TCP phase and the amount of β-TCP in the CaP coating increases with increasing depositing voltages.

The cathode reactions of electrodeposition CaP phases on the surface of magnesium alloy are generally suggested as follows:

$$2H_2O + 2e^- \rightarrow H_2 \uparrow + 2OH^- \tag{1}$$
$$2H_2PO_4^- + 2e^- \rightarrow 2HPO_4^{2-} + H_2 \uparrow \tag{2}$$
$$2HPO_4^{2-} + 2e^- \rightarrow 2PO_4^{3-} + H_2 \uparrow \tag{3}$$

Supersaturated electrolytes buffered at pH=4 have been used for depositing CaP coatings. In the electrolyte, reactions (1) and (2) mainly occured and generated HPO_4^{2-} would partially be deoxidized to PO_4^{3-}, as shown in reaction (3).

During deposition, Ca^{2+} ion will precipitate with HPO_4^{2-} and PO_4^{3-} anions to form CaHPO4 · 2H$_2$O (DCPD) and $Ca_3(PO_4)_2$ (β-TCP), respectively:

$$Ca^{2+} + HPO_4^{2-} + 2H_2O \rightarrow CaHPO_4 \cdot 2H_2O \tag{4}$$
$$3Ca^{2+} + 2PO_4^{3-} \rightarrow Ca_3(PO_4)_2 \tag{5}$$

These reactions are considered to be the ones having a major effect on the formation of calcium phosphates because of their active role in controlling the pH and producing hydroxyl ions.
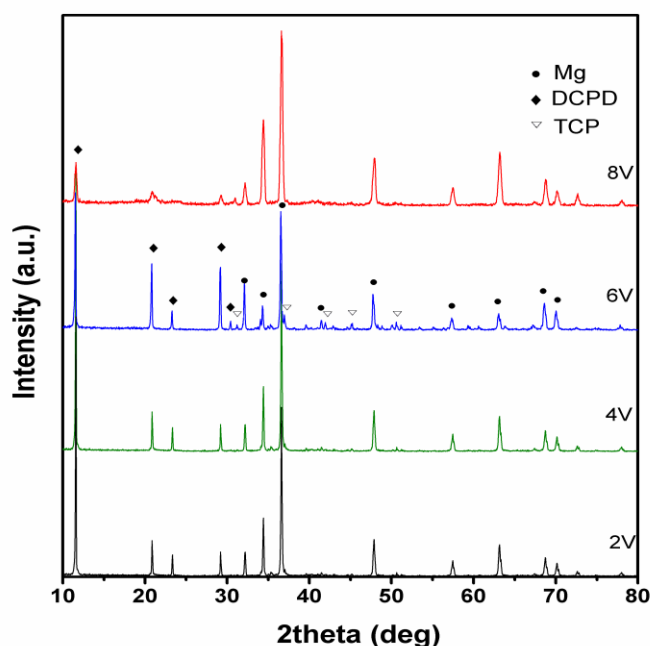
Figure 1. XRD patterns of ZK60 alloys with CaP coatings electrodeposited at different voltages

Figure.2 shows the surface morphology (SEM) of the electrodeposited CaP coatings at different voltages. It was found that a homogenous coating layer was formed on the surfaces of the substrate. Most of the as-deposited coating shows dendritic morphology with a lot of flakes and fine crystal size, which is similar to the DCPD coating that is prepared by electrodeposition in Song's study [23]. For the coating electrodeposited at 2V, a dendritic structure, composed of regular flakes which were about 2-5 μm in thickness and 50-100 μm in length, was observed in the coating, and the flakes aggregate closely. When the electrodeposition voltage is increased to 4V and 6V, the coatings still show dendritic morphology but the size of flakes is increased apparently. Further increasing the deposition voltage to 8V, the surface morphology changes significantly. There is no dendritic structure can be observed in the coating, but a kind of rod-like structure with size of about 50-100 μm in length is seen.
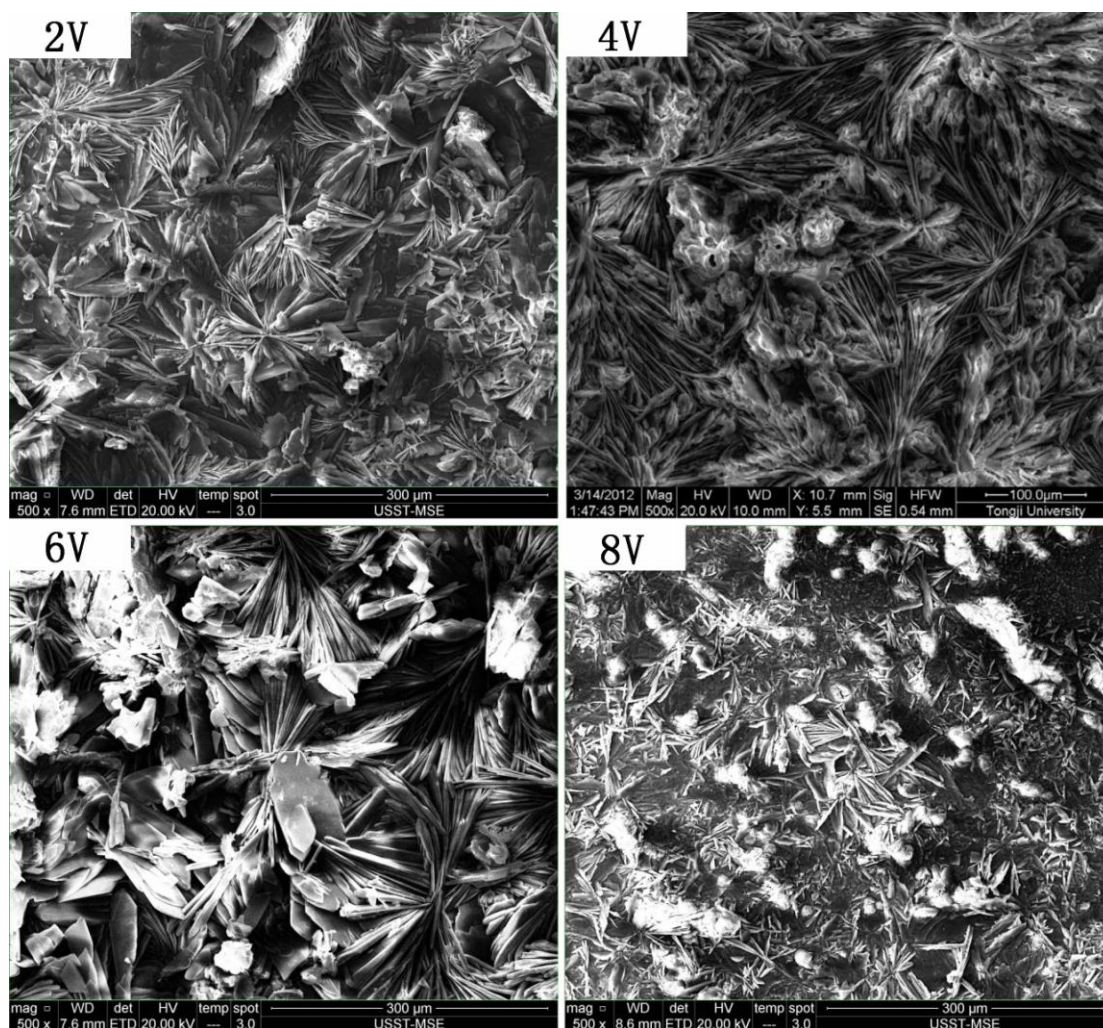
Figure 2. SEM morphologies of coated samples.

The compositions of the coatings were examined by EDS, as shown in Fig.3. The main elements detected on the surface of the coatings were Ca, P, C, and O indicating that CaP phase was present in the coating. EDS analysis of the various coatings revealed that Ca/P atomic ratio was found to be around 0.89, 0.88, 0.93 and 0.83 for coatings deposited at voltage of 2V, 4V, 6V and 60 °C, respectively. It seems that deposition voltage has little influence on the Ca/P ratio. The Ca/P ratios of

all the coatings are close to that of the stoichiometric DCPD (1). This result indicates that our DCPD coating is calcium-deficient. This is due to substitutions in the lattice. Calcium phosphate compounds can be substituted with different ions. In the DCPD lattice, calcium can be replaced by small amounts of magnesium and sodium, and phosphates can be replaced by carbonate ions. During the electrodepositing process, these ions are incorporated into the coating. It is also known that there may be a significant amount of magnesium incorporated into coatings which makes calcium magnesium brushite the mostly like phase present due to the corrosion of the substrate during the coating process.
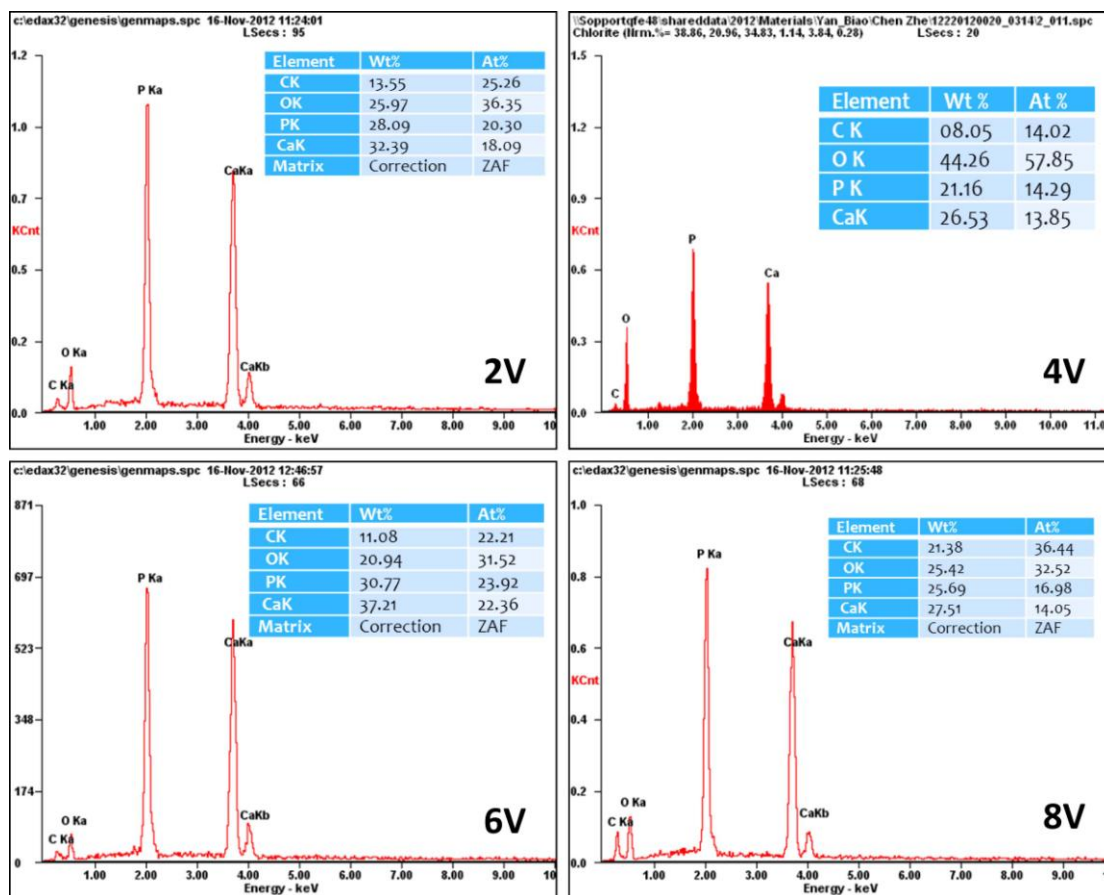

Figure 3. EDS patterns of coated samples.

The Tafel curves obtained for CaP-coated and uncoated ZK60 alloy samples in SBF solution at 37°C were plotted based on the electrochemical characterizations, as shown in Fig.4. Generally, the Tafel curves are assumed to represent the cathodic hydrogen evolution through water reduction, while the anodic ones represent the dissolution of magnesium. The cathodic parts of the curves in Fig. 4 indicate that the cathodic polarization current of the hydrogen evolution reaction on the DCPD-coated Mg alloy is much higher than that on the uncoated Mg substrate. That is to say, the overpotential of the cathodic hydrogen evolution reaction is lower on the DCPD-coated Mg alloy than on the uncoated Mg substrate. This also reveals that the cathodic reaction is easier kinetically on the DCPD-coated specimen than on the bare one, which may be due to the existence of the DCPD coating. Tafel-type analysis was performed on the linear regions of the plot, using the Tafel slopes from between 50 and 250mV away from the corrosion potential, to provide an approximation of the corrosion current

density. Values of the corrosion potential E_{corr} and the corrosion current density I_{corr} were extracted from these curves and are shown in Table 2. The initial corrosion potential (E_{corr}) of the DCPD-coated Mg alloy samples were all higher than the uncoated alloy sample (-1.53V). While the corrosion current density I_{corr} is about 2-3 order of magnitude lower than that of the uncoated magnesium. This result further indicates that the corrosion resistance of magnesium has been improved by the DCPD coating. The lower corrosion current density was due to the smaller portion of exposed area to the solution. Thus, there was a decrease in anodic reaction rate (the corrosion rate). The coating decreases the available surface area susceptible to corrosion. The corrosive solution cannot attack the magnesium where it is protected by the CaP coating. This matched with the immersion testing results that the initial degradation rate of the CaP-coated samples was lower than the uncoated ones. In all the samples, the sample coated at 4V has the best in vitro corrosion resistance. From the results of electrochemical testing analysis, it is obvious that the Ca-P coating could improve effectively corrosion resistance of the ZK60 alloy in the SBF solution. The improvement in corrosion resistance will greatly reduce the initial biodegradation rate of the implants, and is essential for maintaining the implant's mechanical strength in the bone reunion period. In terms of the design of degradable implants, this means that a thinner or less bulky bone plate could be used compared with untreated Mg implants having the same service life.

Table 2. Corrosion parameters obtained from electrochemical analysis

samples	E_{corr} (V)	I_{corr} (A)
uncoated	-1.531	1.768e-004
2V	-1.370	5.358e-006
4V	-1.280	1.977e-006
6V	-1.325	1.279e-006
8V	-1.393	3.466e-007
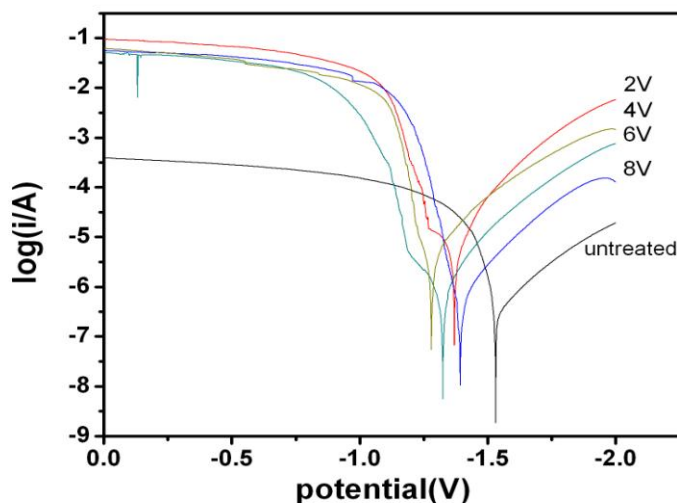
Figure 4. Tafel plot of the samples in SBF solution

To examine the long-term corrosion behavior, the in vitro corrosion behavior of the CaP-coated and uncoated ZK60 alloy samples in SBF were monitored. The pH values of the SBF were monitored every day during the sample immersion. Fig.4 shows the variation of the pH value of SBF solution at different immersion time. It can be seen that the pH values of the solution with the coated samples increase more slowly than that of the solution with untreated samples in the first 24 hrs. As it is known that the increase of the pH values in Hank's solution mainly results from the dissolution of Mg and the formation of corrosion product $Mg(OH)_2$, it can be concluded that the corrosion rate of coated samples is lower than that of untreated samples. The corrosion rate of Mg alloys during the early stages of implantation would play a critical role in the initial surrounding tissue response. If the initial degradation of Mg-based implants was too rapid, osteolysis would occur, thus adversely affecting bone tissue regeneration.[24] Therefore, it was critical to control and decrease the initial degradation rate. From Fig.4, it can be seen that there is an increase in pH value for all the samples with increasing time. At the first day, the pH value increases sharply for all the samples because of the increase of OH^- concentration caused by the release of Mg^{2+} [25]. The pH for the uncoated sample increases from 7.4 to 8.5 while the pH of coated samples increase only about 0.2~0.4 (The relatively lower increases in pH in current study compared to previous studies [12, 13] are because that only one surface of the samples is exposed to the SBF solution). After 2 days' immersion, the pH changes for all samples slow down. It is clear that the pH change for the uncoated sample was the highest and the pH value reaches to about 10 while the pH values of the solution immersed with CaP coated samples are around 8.4, which is much lower than that of uncoated samples. Therefore, it can be concluded that the samples coated with CaP have a better corrosion resistance than uncoated sample.
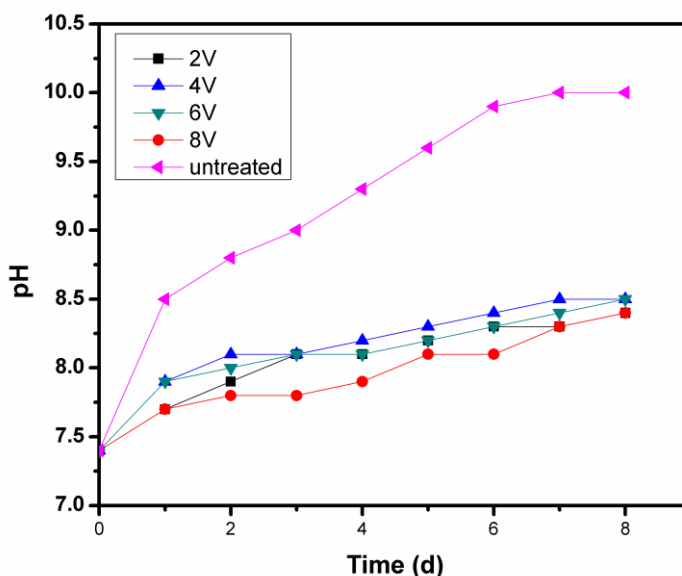

Figure 4. Relationship of sample weight versus immersion time

Fig.5 shows the relationship of sample weight versus immersion time. It was observed that the weight of coated samples do not change much and keep almost constant (there are a little bit increase) with increasing immersion time while that of uncoated sample decreases significantly. The weight

change of the samples immersed in SBF solution was a result of the following three processes: (1) the corrosion of magnesium, (2) the precipitation of CaP coating, and (3) the dissolution of CaP coating. The corrosion of magnesium occurred for all the samples, but their corrosion rates were significantly different owing to varied surface coatings applied to the substrate, including no coating and coating at different voltages.
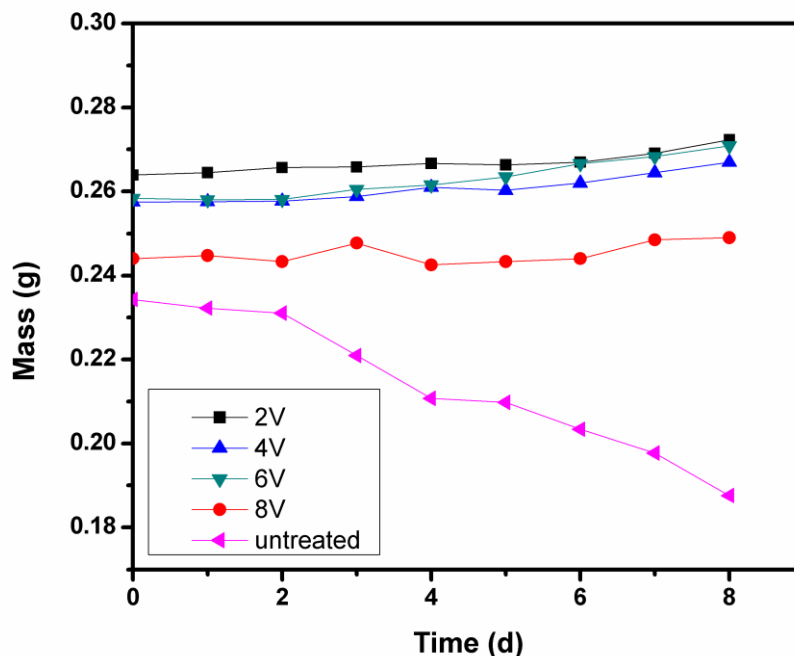

Figure 6. Variation of the pH value of SBF solution at different immersion time

4. CONCLUSIONS

In summary, CaP coating was successfully prepared on the ZK60 magnesium by electrodeposition. The CaP coatings show a DCPD phase structure with small amount of β-TCP phase. The surface morphology shows a typical dendritic structure and the deposition voltage has little influence on the Ca/P ratio. The corrosion resistance of ZK60 alloy is obviously improved after coated with CaP coatings and the sample with CaP coating deposited at 4V has the best corrosion resistance. The improvement in corrosion resistance will greatly reduce the initial biodegradation rate of the implants, and is essential for maintaining the implant's mechanical strength in the bone reunion period. Thus ZK60 alloy coated with the Ca-P coating prepared in this study is a promising candidate for biodegradable orthopedic implant.

References

1. Mark P. Staiger, Alexis M. Pietak, Jerawala Huadmai, George Dias. *Biomaterials,* 27 (2006) 1728–1734
2. Frank Witte, Norbert Hort, Carla Vogt, Smadar Cohen, Karl Ulrich Kainer,Regine Willumeit, Frank Feyerabend. *Current Opinion in Solid State and Materials Science,* 12 (2008) 63–72
3. C. R. Howlett, H. Zreioat, R. O'Dell, J. Noorman, P. Evans, B. A. Dalton, C. McFarland, J. G. Steele, *J. Mater. Sci: Mater. Med.*, 5 (1994) 715-722.
4. B.A. Shaw. Corrosion resistance of magnesium alloys. In: Stephen D, editor. ASM handbook volume 13a: Corrosion: fundamentals, testing and protection. UK: ASM International; 2003.
5. F. Witte, V. Kaese, H. Haferkamp, E. Switzer, A. Meyer-Lindenberg, C.J. Wirth, et al. *Biomaterials*, 26(2005) 3557–3563.
6. F. Witte, J. Fischer, J. Nellesen, H.A. Crostack, V. Kaese, A. Pisch, et al. *Biomaterials* 27(2006) 1013–1018.
7. F. Witte. *Acta Biomaterialia*, 6 (2010) 1680–1692.
8. Li KaiKai, Wang Bing, Yan Biao, Lu Wei. *J. Biomater. Appl.*, doi: 10.1177/0885328212453958
9. Jingxin Yang, Fuzhai Cui, and In Seop Lee. *Annals of Biomedical Engineering*, 39, (2011) 1857–1871
10. Li KaiKai, Wang Bing, Chai Jing, Yan Biao & Lu Wei. *Sci. China Tech. Sci.,* 56 (2013) 80-83
11. Wei Lu, Zhe Chen, Ping Huang and Biao Yan. *Int. J. Electrochem. Sci.,* 8 (2013) 9518 - 9530
12. Wei Lu, Zhe Chen, Ping Huang and Biao Yan. *Int. J. Electrochem. Sci.,* 7 (2012) 12668 - 12679
13. Li KaiKai, Wang Bing, Yan Biao & Lu Wei. *Chin. Sci. Bull.,* 57 (2012) 2319-2322
14. Pamela Habibovic, Florence Barre`re, Clemens A. van Blitterswijk, Klaas de Groot, and Pierre Layrolle. *J. Am. Ceram. Soc.*, 85 (2002) 517–22
15. Tal Reiner, Leonid M. Klinger, and Irena Gotman. *Crystal Growth & Design*, 11 (2011) 190–195
16. Shaylin Shadanbaz , George J. Dias. *Acta Biomaterialia*, 8 (2012) 20–30
17. M.C. Kuo, S.K. Yen. *Mater. Sci. Eng. C*, 20 (2002) 153–160
18. M. Ma, W. Ye, X.-X. *Wang. Mater. Lett.*, 62 (2008) 3875–3877
19. D.J. Blackwood, K.H.W. Seah. *Mater. Sci. Eng. C*, 29 (2009) 1233–1238
20. E.C. Meng, S.K. Guan, H.X. Wang, L.G. Wang, S.J. Zhu, J.H. Hu, C.X. Ren, J.H. Gao, Y.S. Feng. *Applied Surface Science*, 257 (2011) 4811–4816
21. M. Bobby Kannan. *Materials Letters*, 76 (2012) 109–112
22. M. Bobby Kannan, O. Wallipa. *Materials Science and Engineering C*, 33 (2013) 675–679
23. Y. Song, S.X. Zhang, J.N. Li, C.L. Zhao, X.N. Zhang. *Acta Biomaterialia*, 6 (2010) 1736–1742
24. R. G. Guan, I. Johnson, T. Cui, T. Zhao, Z. Y. Zhao, X. Li, H. Liu, *J. Biomed Mater Res A.*, 100 (2012) 999-1015
25. A. Atrens, M. Liu, N. I. Z.l Abidin, *Materials Science and Engineering B*, 176 (2011) 1609-1636